

Three-dimensional vortex dynamics in Bose-Einstein condensates

B. M. Caradoc-Davies, R. J. Ballagh, and P. B. Blakie

Department of Physics, University of Otago, P. O. Box 56, Dunedin, New Zealand.

(March 6, 2000)

We simulate in the mean-field limit the effects of rotationally stirring a three-dimensional trapped Bose-Einstein condensate with a Gaussian laser beam. A single vortex cycling regime is found for a range of trap geometries, and is well described as coherent cycling between the ground and the first excited vortex states. The critical angular speed of stirring for vortex formation is quantitatively predicted by a simple model. We report preliminary results for the collisions of vortex lines, in which sections may be exchanged.

PACS numbers: 03.75.Fi, 47.32.Cc

The formation and properties of vortices in Bose-Einstein condensates are attracting intense current interest. A number of schemes for producing vortices in trapped condensates have been proposed theoretically, and the first experimental creation of a topological vortex in a two-component condensate has been reported [1], in agreement with a numerical model [2]. Simulations of flow of a condensate past a spherical object have shown vortex ring solutions [3], and numerical studies of vortex formation in rotating traps have shown the formation of vortex arrays [4]. Very recently the first report has been made of the observation of vortices in a single-component condensate [5].

In an earlier paper [6], we showed that a rotationally stirred Bose-Einstein condensate, simulated in two dimensions, exhibits a simple single vortex cycling regime, a behaviour we described as nonlinear Rabi cycling. In the present paper we demonstrate that the single vortex cycling regime is also found in full three-dimensional simulations of condensate stirring (as shown in Fig. 1), in a parameter regime accessible to current experiments. The single vortex regime is studied in a variety of trap geometries (oblate to prolate) as is the dynamical stability of central vortices. The line character of a vortex in three dimensions also gives rise to some qualitatively new behaviour that has no analogue in two dimensions. We show that in a spherical trap, stirring of the condensate can produce two vortex lines which collide and exchange sections.

As in the earlier work, our treatment is based on the time-dependent Gross-Pitaevskii (GP) equation,

$$i \frac{\partial \psi(\mathbf{r}, t)}{\partial t} = [-\nabla^2 + V(\mathbf{r}, t) + C|\psi(\mathbf{r}, t)|^2] \psi(\mathbf{r}, t), \quad (1)$$

in dimensionless units [7]. The total external potential $V(\mathbf{r}, t)$ is given by $(x^2 + y^2 + \lambda^2 z^2)/4 + W(\mathbf{r}, t)$, where the first term represents a cylindrically symmetric trap with trap anisotropy parameter λ . The second term $W(\mathbf{r}, t)$ is the contribution of the stirrer, a far-blue detuned Gaussian laser beam cylindrically symmetric about a line parallel to the z axis,

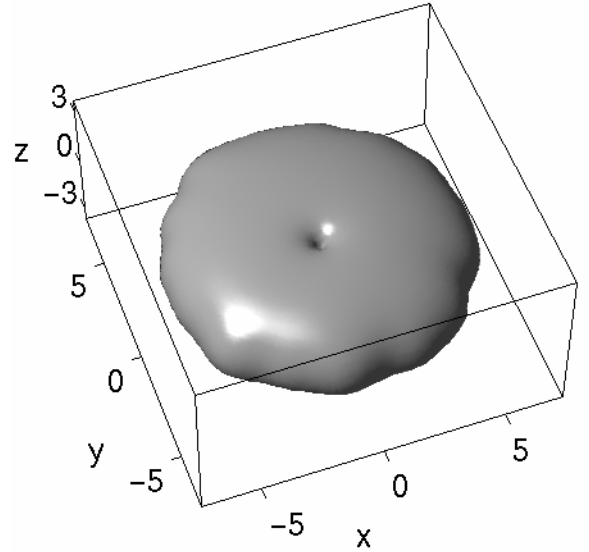


FIG. 1. Probability density isosurface ($|\psi|^2 = 10^{-4}$) for a condensate stirred as described in the text, with the stirrer linearly withdrawn between $t = 7\pi$ and $t = 8\pi$. Here $t = 94.12$, and the hole near the centre of the condensate is a vortex that has been drawn in from the edge and remains close to the centre of the condensate. Parameters are $C = 1000$, $\lambda = \sqrt{8}$, $W_0 = 4$, $w_s = 4$, and $\rho_s = 2$. The angular frequency of stirring $\omega_f = 0.3$ is less than the critical frequency $\omega_c = 0.323$.

$$W(\mathbf{r}, t) = W_s(t) \exp \left[- \left(\frac{|\boldsymbol{\rho} - \boldsymbol{\rho}_s(t)|}{w_s/2} \right)^2 \right], \quad (2)$$

where $\boldsymbol{\rho}$ is the projection of \mathbf{r} into the $z = 0$ plane, and $\boldsymbol{\rho}_s$ is the centre of the Gaussian stirrer in that plane.

The condensate is stirred in a manner similar to our earlier work [6], with the stirrer moving in a circle of radius ρ_s at a constant angular velocity ω_f . Here, however, we begin with the ground state of the harmonic trap (with no stirrer present), and minimise transient effects by increasing the stirrer amplitude W_s linearly from zero to a final value of W_0 between $t = 0$ and $t = \pi$. With

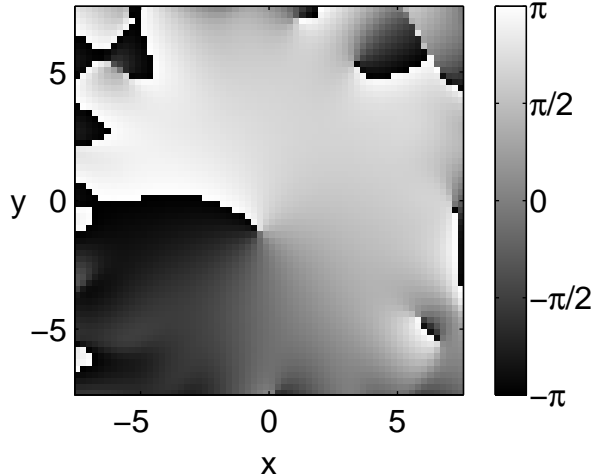


FIG. 2. Phase of ψ in the $z = 0$ plane for the condensate shown in Fig. 1.

an appropriate choice of parameters, as in Fig. 1, a single vortex with positive circulation is drawn close to the centre of the condensate, and for continuous stirring cycles in and out. This is exactly the behaviour found previously in a two-dimensional system [6], and in fact the parameter choice for the single vortex cycling behaviour in three dimensions is guided by the same considerations outlined there, as we discuss below. Figure 2, where we plot the phase of the wavefunction, shows that the central feature of Fig. 1 is a vortex of positive circulation. In Fig. 3 the evolution of the angular momentum expectation value (which in our dimensionless units is 0 for the ground state and 1 for the central vortex state) is presented and confirms that for continuous stirring (thin line), the vortex cycles in and out of the condensate.

In contrast to the two-dimensional case, the three-dimensional simulation can be unambiguously related to a realistic current experimental scenario. The $C = 1000$ case shown in Figs. 1–3 corresponds to $N = 1.8 \times 10^4$ atoms of ^{87}Rb in the $|F = 2, m_f = 2\rangle$ hyperfine state (for which we use an s-wave scattering length $a = 5.29$ nm) in a time orbiting potential (TOP) trap with radial trap frequency $\omega_r = 2\pi \times 15$ Hz and $\lambda = \omega_z/\omega_r = \sqrt{8}$. For this example, our computational units of time and length [7] correspond to 10.6 ms and $1.97 \mu\text{m}$ respectively, and the Thomas-Fermi diameter of the condensate in the radial direction of 11.7 corresponds to about $23 \mu\text{m}$. The stirrer Gaussian $1/e$ diameter $w_s = 4$ corresponds to a Gaussian $1/e^2$ beam diameter of approximately $11 \mu\text{m}$. The required intensity of the stirring laser is detuning dependent, but can be easily calculated from the light shift potential $\hbar\Omega^2/4\Delta$, where Ω and Δ are the Rabi frequency and detuning respectively of the atom-laser interaction. For example, if the laser beam is 50 nm blue-detuned from the 780 nm atomic transition, $\Delta = 1.65 \times 10^{14} \text{ s}^{-1}$, and a laser power of 300 nW is required for the 3 nK

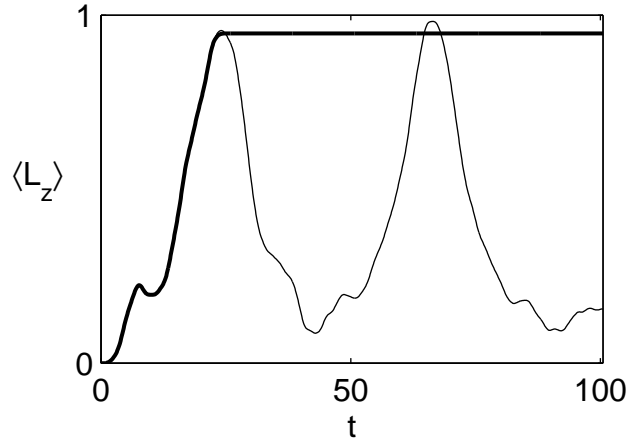


FIG. 3. Condensate angular momentum expectation value versus time, for the case of a constantly rotating stirrer (thin line), or stirrer linearly withdrawn between $t = 7\pi$ and $t = 8\pi$ (thick line). Parameters as in Fig. 1.

height stirrer we describe. The first angular momentum peak in Fig. 3 occurs at 0.26 s, which is much less than the lifetime of the condensate. The occurrence of the single vortex cycling behaviour in this experimentally accessible parameter regime suggests a method of preparing a central vortex state; stir the condensate as we have described, then remove the stirrer at the time when the angular momentum peak is expected. We illustrate the implementation of this method in Fig. 3 with the thick curve, for which the stirrer is linearly withdrawn between $t = 7\pi$ and $t = 8\pi$. Once the stirrer is removed, the vortex remains in the condensate, circling about and close to the centre, and $\langle L_z \rangle$ is constant.

The vortex cycling behaviour illustrated by the example in Figs. 1–3 indicates that the two-state model described in our earlier work (for the two-dimensional case [6]) also has application in three-dimensions. Here we briefly outline the modifications required to extend the two-state model into three dimensions. We represent the condensate by an axisymmetric component ϕ_s , and a vortex-like component $\phi_v e^{i\theta}$ which has a circulation about the z axis, where ϕ_s and ϕ_v are real and nonnegative, so

$$\psi(\mathbf{r}, t) = a_s(t)\phi_s(\rho, z, n_v) + a_v(t)\phi_v(\rho, z, n_v)e^{i\theta}, \quad (3)$$

with $\rho = \sqrt{x^2 + y^2}$. We choose ϕ_s and ϕ_v to satisfy the following time-independent coupled equations,

$$\mu_s \phi_s = \left[-\frac{1}{\rho} \frac{d}{d\rho} \left(\rho \frac{d}{d\rho} \right) - \frac{d^2}{dz^2} + \frac{\rho^2 + \lambda^2 z^2}{4} + C(n_s \phi_s^2 + 2n_v \phi_v^2) \right] \phi_s, \quad (4a)$$

$$\mu_v \phi_v = \left[-\frac{1}{\rho} \frac{d}{d\rho} \left(\rho \frac{d}{d\rho} \right) - \frac{d^2}{dz^2} + \frac{1}{\rho^2} \right] \phi_v,$$

$$+ \frac{\rho^2 + \lambda^2 z^2}{4} + C (n_v \phi_v^2 + 2n_s \phi_s^2) \Big] \phi_v, \quad (4b)$$

where the eigenvalues μ_s and μ_v are found by solving Eqs. (4b) for a given choice of the vortex fraction $n_v = |a_v|^2$. The quantity $n_s = |a_s|^2 = 1 - n_v$. We note that when $n_v = 0$, Eqs. (4) reduce to Eq. (4a), the time-independent GP equation for the ground state, while if $n_v = 1$, Eqs. (4) reduce to Eq. (4b), the time-independent GP equation for the first excited vortex. The resulting nonlinear Rabi equations for the two-state system [obtained by substituting Eq. (3) into Eq. (1)] are then identical in form to Eqs. (5–6) of [6], but with the wavefunctions ϕ_s and ϕ_v now defined over ρ and z instead of r .

The underlying assumption of our two-state model is that the ground state (or more generally, ϕ_s) is coupled primarily to the vortex state of lowest energy with axis parallel to the stirrer axis. In two dimensions, there are a limited number of excited condensate states in the appropriate energy range that can be coupled to the symmetric state by the stirring potential, and we have previously shown [6] that the two state model works well within a specified validity range. In three-dimensional cylindrically symmetric traps, many more condensate eigenstates exist, and although symmetry considerations limit the possible coupling from the symmetric state, a two state model places more constraint on the description of the system than in the two-dimensional case. We do not aim therefore to provide a detailed representation of the stirring behaviour with our two state model, instead we use it primarily to provide conceptual understanding of the cycling behaviour. Nevertheless we also find it gives a quantitatively accurate prediction of the critical frequency of rotation ω_c , the stirring frequency which causes a single vortex to cycle right to the centre of the condensate. We have examined the single vortex cycling behaviour using the full GP solution, for a variety of trap geometries including the oblate ($\lambda = \sqrt{8}$), spherical ($\lambda = 1$), and prolate ($\lambda = 1/3$) cases, with a condensate of $C = 1000$, and a stirring potential of the same size and position as in Fig. 1. We find that the critical rotational frequency for single vortex cycling is accurately predicted by the two state model as the difference in energy between the ground and vortex states of the condensate (modified by the finite size of the stirrer, see Eq. (7) of [6]). As in [6], a sufficiently large Rabi frequency is required to distort the energy barrier between ground and vortex state enough to permit cycling. When the critical frequency of rotation is exceeded, additional vortices penetrate the condensate.

It is worth noting that as the z component of the trapping potential become weaker (that is, as λ becomes smaller), then in addition to the vortex state, the stirring potential increasingly excites the dipole (centre of mass) oscillation of the condensate. This can be understood in terms of the Ehrenfest theorem: for our choice of parameters the mean force $\langle -\nabla W \rangle$ of the stirrer increases as

the condensate radial size decreases because the condensate is increasingly concentrated near the steepest part of the stirring potential. The centre of mass motion contributes angular momentum $\langle L_z \rangle_{COM}$ to the condensate angular momentum, where

$$\langle L_z \rangle_{COM} = \langle x \rangle \langle P_y \rangle - \langle y \rangle \langle P_x \rangle. \quad (5)$$

We find that $\langle L_z \rangle - \langle L_z \rangle_{COM}$ (which is a measure of the angular momentum caused by the presence of the vortex) for all three trap geometries cycles between 0 and 1 when ω_f is slightly less than ω_c (the single vortex cycling regime) and oscillates about 1 when ω_f just exceeds ω_c (and multiple vortices penetrate the condensate). $\langle L_z \rangle_{COM}$ is small for the $\lambda = \sqrt{8}$ case shown in Fig. 3.

If the single stirrer used in Fig. 1 is replaced by two stirrers of half the height but on opposite sides of the z axis, no vortex cycling occurs, and $\langle L_z \rangle$ exhibits only small oscillations of amplitude less than 0.04. This is easily understood from our two state model, because the Rabi frequency Ω (see Eq. (6b) of [6]) is zero for this stirrer configuration, as it is for any stirrer configuration of even symmetry. It is worth pointing out that our scenario of coherent cycling should be distinguished from vortex production by damping in a trap with a symmetric rotating distortion, such as the recently reported experiment [5], or numerical damping schemes such as imaginary-time propagation [4].

Our three-dimensional simulations also allow us to test (in the mean-field limit) the stability of pure vortex eigenstates. Using as an initial state a central vortex (an eigenstate of the time-independent GP equation) for $C = 1000$, a perturbation was applied by linearly inserting and withdrawing (between $t = 0$ and $t = \pi$) a stirrer of the same size as in Fig. 1 but at a fixed position in the laboratory frame. We find that for a range of trap geometries ($\lambda = \sqrt{8}$, 1, or $1/3$), the $\langle L_z \rangle = 1$ vortex is dynamically stable, and remains near the centre of the condensate. We can understand this result in terms of Rabi cycling. The stationary stirrer ($\omega_f = 0$) provides a potential which is far-detuned from resonance ($\omega_f = \omega_c$), and thus there is a low probability of transfer out of the initial (vortex) state. Indeed if the stirrer remains fixed in the condensate after insertion and is not withdrawn, we find that the vortex still remains near the centre of the condensate and follows a small closed path displaced slightly away from the stirrer. By contrast, for these geometries, the $\langle L_z \rangle = 2$ central vortex eigenstate immediately dissociates into two unit vortices when perturbed. We note that these stability results refer to dynamical stability in the GP limit (that is, $T = 0$), as opposed to thermodynamic stability [8,9].

In addition to confirming the basic features of the two state model of vortex cycling, our three-dimensional simulations also reveal some new phenomena. The vortices produced in three dimensions by stirring are line vortices. In the $\lambda = \sqrt{8}$ configuration, the lines are nearly

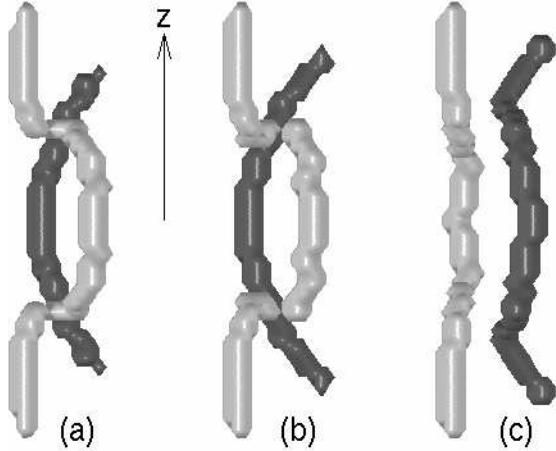


FIG. 4. Collision of vortex lines and exchange of sections in a stirred condensate. View is from a position in the $z = 0$ plane, looking almost down the $y = -x$ line. In (a) $t = 6.79$, (b) $t = 6.91$, and (c) $t = 7.04$. Parameters are the same as in Fig. 1 except that $\lambda = 1$. The angular frequency of stirring $\omega_f = 0.45$ exceeds the critical frequency $\omega_c = 0.399$.

straight and parallel to the stirrer axis, and when two lines of the same circulation form, we find they repel each other. For a spherical trap ($\lambda = 1$) however, vortex lines along any direction are degenerate (in the absence of the stirrer) with the vortex eigenstate about the z axis. Accordingly, the vortex lines can become more curved than in the oblate case, as we find in our simulations below the critical frequency, where the vortex that forms can have appreciable curvature. Above the critical frequency, when multiple vortices are drawn into the condensate, there is a striking consequence of this potential for vortex lines to deform. In a collision between two such curved vortex lines, sections of the lines can be exchanged, as we show in the collision sequence in Fig. 4. The condensate is stirred somewhat above the critical frequency in a spherical trap, and by $t = 6.79$ two vortex lines (both of positive sense [10]) have formed. The figure shows only the vortex lines (detected numerically), which have been shaded light and dark to distinguish one from the other. In Fig. 4(a) the dark vortex line approaches the light vortex line from behind, and because of their mutual repulsion, the light line has developed a bulge. In Fig. 4(b) the dark line is now close to the light line, causing the bulge to become recurved, with two small portions now nearly antiparallel to the dark line. In Fig. 4(c) the two lines have completed a collision and exchanged their central sections.

In conclusion, we have shown that the single vortex cycling regime we discovered previously in simulations of two-dimensional condensates is also present in three-dimensional condensates, for a range of trap geometries. We have related our simulations to current experimental configurations, and have demonstrated how the cy-

cling behaviour could be used to generate a central vortex state. We have investigated the dynamical stability of central vortex states, and have also given initial evidence of the rich dynamical behaviour of vortex lines.

This work was supported by the Marsden Fund of New Zealand under contract PVT902.

-
- [1] M. R. Matthews *et al.*, Phys. Rev. Lett. **83**, 2498 (1999).
 - [2] J. E. Williams and M. J. Holland, Nature **401**, 568 (1999).
 - [3] T. Winiiecki, J. F. McCann, and C. S. Adams, Europhys. Lett. **48**, 475 (1999).
 - [4] D. L. Feder, C. W. Clark, and B. I. Schneider, Phys. Rev. A **61**, 011601(R) (2000).
 - [5] K. W. Madison, F. Chevy, W. Wohlleben, and J. Dalibard, Phys. Rev. Lett. **84**, 806 (2000).
 - [6] B. M. Caradoc-Davies, R. J. Ballagh, and K. Burnett, Phys. Rev. Lett. **83**, 895 (1999).
 - [7] Our units of time and length are ω^{-1} and $(\hbar/2m\omega)^{1/2}$ respectively, where ω is the trap frequency in the x direction. The nonlinearity parameter $C = 8\pi aN(2m\omega/\hbar)^{1/2}$ and we normalise the wavefunction by $\int |\psi(\mathbf{r}, t)|^2 d\mathbf{r} = 1$.
 - [8] D. S. Rokhsar, Phys. Rev. Lett. **79**, 2164 (1997).
 - [9] A. L. Fetter, J. Low Temp. Phys. **113**, 189 (1998).
 - [10] Positive sense here means that following from the bottom to the top the direction of circulation is given by the right hand rule.